Chapter 15

Linear Controller Design for the NEC Laser Bonder via Linear Matrix Inequality Optimization

Junichiro Oishi and Venkataramanan Balakrishnan

15.1 Introduction

Over the past few decades, rapid strides have been made in control theory, resulting in the solution of several important controller design problems: LQR, LQG, $\mathbf{H}_\infty$, to name a few [17, 10, 13]. Many of these controllers have been successfully implemented in industrial applications. However, a disadvantage with most of these methods is that they are optimal in only a narrow sense, and actual engineering specifications (which are usually stated as competing constraints) must be translated or reinterpreted so as to fit into the narrow framework of these methods.

In parallel with the theoretical developments in systems and control, there have been significant advances in optimization theory and algorithms, as well as an almost exponential growth in computing power, so that *numerical* controller design methods, especially those based on convex optimization, have become increasingly relevant [3, 7, 5, 4, 15, 16, 2]. Such numerical methods enjoy the advantage that several commonly encountered design requirements can be specified directly in a natural manner and that the design interaction between various competing performance specifications can be readily studied. In this chapter, we describe the application of one such computer-aided design method for controlling the NEC Laser Bonder. This method combines the Youla parametrization of the set of achievable stable closed-loop maps with convex optimization based on linear matrix inequalities (LMIs) to numerically design optimal linear time-invariant (LTI) controllers under multiple design specifications.

The significance of Youla parametrization for computer-aided control system design has long been recognized; see, for example, [3, 4]. In these references, the Youla parametrization is used to reformulate the problem of LTI controller design for LTI systems as a quadratic programming problem, which is then solved numerically. The approach that we present in this chapter is very close in spirit to the one in [3, 4]. The main difference is that here the LTI controller design problem is reformulated instead as an LMI optimization problem; we describe this reformulation in section 15.2. We apply this technique, in section 15.3, to design an LTI controller for the NEC Laser Bonder.

15.2 Controller design using the Youla parametrization and LMIs

A standard framework for controller design is shown in Figure 15.1. The time index is discrete. P is the model of the plant, i.e., the system to be controlled. K is the controller that implements the control strategy for improving the performance of the system. y is the signal that the controller has access to, and u is the output of the controller that drives the plant. w and z represent inputs and outputs of interest. Note that z can include components of the control input u, so that specifications on the control input such as bounds on the control effort can be handled. In other words, the map H_{zw} from w to z contains all the input–output maps of interest. The controller design problem is the design of an LTI controller K such that the closed-loop map H_{zw}, with the controller K in place, satisfies some design specifications. Often an "optimal" controller is sought, one that yields an optimal performance measure subject to the design specifications.

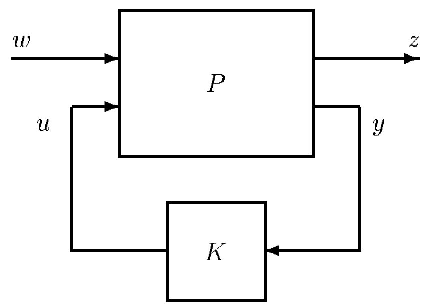

FIG. 15.1. *A standard controller design framework.*

The Youla parameterization (see [18] for details) yields a *convex* (in particular *affine*) parameterization, in terms of the Youla parameter Q, of the set of achievable stable closed-loop maps H_{zw} from w to z for the system in Figure 15.1. This fact is of great significance, as the numerical search for the "optimal" Youla parameter Q—one that minimizes an objective that is a convex function of H_{zw} subject to convex constraints on H_{zw}—is a *convex optimization problem*. In this section, we show how by restricting Q to lie in a finite-dimensional subspace, we can reformulate several important practical controller design specifications as LMI constraints on Q. Some of the design specifications that we will consider are constraints on the response z for some reference input w, asymptotic tracking constraints, bounds on the $\mathbf{H}_2$ and $\mathbf{H}_\infty$ norms of H_{zw}, etc. Thus several important LTI controller design problems can be solved numerically using optimization over LMIs.

15.2.1 Youla parametrization

We begin with a brief review of the Youla parametrization of the set of achievable stable closed-loop maps for LTI plants with LTI controllers.

Let the state equations describing the plant P be

$$\begin{aligned} x(k+1) &= Ax(k) + B_w w(k) + B_u u(k), \\ z(k) &= C_z x(k) + D_{zw} w(k) + D_{zu} u(k), \\ y(k) &= C_y x(k) + D_{yw} w(k) + D_{yu} u(k). \end{aligned}$$

Let the open-loop plant transfer matrix in Figure 15.1, denoted P, be partitioned as

$$P = \begin{bmatrix} P_{zw} & P_{zu} \\ P_{yw} & P_{yu} \end{bmatrix}.$$

Then, with $K(\lambda)$ denoting the transfer function of the LTI controller, the transfer function from w to z is

$$H_{zw}(\lambda) = P_{zw}(\lambda) + P_{zu}(\lambda)K(\lambda)\left(I - P_{yu}(\lambda)K(\lambda)\right)^{-1} P_{yw}(\lambda). \tag{15.1}$$

The set of achievable, stable closed-loop maps from w to z is given by

$$\mathcal{H} = \{H_{zw} : H_{zw} \text{ is stable, and satisfies (15.1) for some } K\}. \tag{15.2}$$

The set of the controllers K that stabilize the system is in general not a convex set. Thus optimizing over $\mathcal{H}$ using the description (15.2), with K as the (infinite-dimensional) optimization variable, is a difficult numerical problem. However, the theory of Youla parameterization enables us to give a convex parameterization of $\mathcal{H}$.

It turns out (see [4] and the references therein for details) that the set $\mathcal{H}$ can be also written as

$$\mathcal{H} = \{H_{zw} : H_{zw}(\lambda) = T_1(\lambda) + T_2(\lambda)Q(\lambda)T_3(\lambda),\ Q \text{ is stable}\},$$

where T_1, T_2, and T_3 are fixed, stable transfer matrices that can be computed as follows.

Let K_{nom} and L_{nom} be real matrices of appropriate sizes such that $A - B_u K_{\text{nom}}$ and $A - L_{\text{nom}}C_y$ are stable (i.e., have all their eigenvalues in the open unit disk). Then T_1, T_2, and T_3 are given by

$$\begin{bmatrix} T_1(\lambda) & T_2(\lambda) \\ T_3(\lambda) & 0 \end{bmatrix} = C_T(\lambda I - A_T)^{-1}B_T + D_T,$$

where

$$A_T = \begin{bmatrix} A_p & -B_u K_{\text{nom}} \\ L_{\text{nom}}C_y & A_p - B_u K_{\text{nom}} - L_{\text{nom}}C_y \end{bmatrix}, \quad B_T = \begin{bmatrix} B_w & B_u \\ L_{\text{nom}}D_{yw} & B_u \end{bmatrix},$$

$$C_T = \begin{bmatrix} C_z & -D_{zu}K_{\text{nom}} \\ C_y & -C_y \end{bmatrix}, \qquad D_T = \begin{bmatrix} D_{zw} & D_{zu} \\ C_{yw} & 0 \end{bmatrix}.$$

The most important observation about this reparametrization of $\mathcal{H}$ is that it is *affine* in the infinite-dimensional parameter Q; it is therefore a convex parameterization of the set of achievable stable closed-loop maps from w to z. (The parameter Q is also referred to as the Youla parameter.) This fact has an important ramification—it is possible now to use convex optimization techniques to find an optimal parameter Q_{opt} and therefore an optimal controller K_{opt}.

The general procedure for designing controllers using the Youla parameterization proceeds as follows. Let ϕ_0, ϕ_1, ..., ϕ_m be (not necessarily differentiable) convex functionals on the closed-loop map that represent performance measures. These performance measures may be norms (typically $\mathbf{H}_2$- or $\mathbf{H}_\infty$-norms), certain time-domain quantities (step response overshoot, steady-state errors), etc.

Then the problem

$$\begin{array}{lll} \text{minimize over } Q: & \phi_0(T_1 + T_2QT_3) \\ \text{subject to} & \phi_1(T_1 + T_2QT_3) \le 0, \\ & \quad\vdots \\ & \phi_m(T_1 + T_2QT_3) \le 0 \end{array} \tag{15.3}$$

is a convex optimization problem (with an infinite-dimensional optimization variable Q). This problem corresponds to minimizing a measure of performance of the closed-loop system subject to other performance constraints.

In practice, problem (15.3) is solved by searching for Q over a finite-dimensional subspace. Typically, Q is restricted to lie in the set

$$\mathcal{Q}_{\text{fin}} = \{Q : Q = \theta_1 Q_1 + \cdots + \theta_N Q_N,\ \ \theta_1, \ldots, \theta_N \in \mathbf{R}\}, \tag{15.4}$$

where $Q_1, \ldots, Q_N$ are fixed, stable transfer matrices. For convenience, we let $\Theta = [\theta_1 \cdots \theta_N]$, and $Q(\Theta) = \theta_1 Q_1 + \cdots + \theta_N Q_N$. This enables us to solve problem (15.3) "approximately" by solving the following problem with a finite number of scalar optimization variables:

$$
\begin{array}{ll}
\text{minimize w.r.t. } \Theta: & \phi_0(T_1 + T_2 Q(\Theta) T_3) \\
\text{subject to} & \phi_1(T_1 + T_2 Q(\Theta) T_3) \le 0, \\
 & \vdots \\
 & \phi_m(T_1 + T_2 Q(\Theta) T_3) \le 0.
\end{array}
\tag{15.5}
$$

The transfer matrices Q_i and their number, N, should be so chosen that the optimal parameter Q can be approximated with sufficient accuracy.

With Θ_{opt} denoting the optimizer of problem (15.5), we can compute optimal controller K_{opt} as follows:

$$K_{\text{opt}}(\lambda) = C_k(\lambda I - A_k)^{-1} B_k + D_k,$$

where

$$A_k = \begin{bmatrix} A_p - B_u K_{\text{nom}} - L_{\text{nom}} C_y - B_u D_Q C_y & B_u C_Q \\ -B_Q C_y & A_Q \end{bmatrix}, \quad B_k = \begin{bmatrix} L_{\text{nom}} + B_u D_Q \\ B_Q \end{bmatrix},$$

$$C_k = \begin{bmatrix} -K_{\text{nom}} - D_Q C_y & C_Q \end{bmatrix}, \qquad D_K = D_Q,$$

and (A_Q, B_Q, C_Q, D_Q) is a realization of $Q(\Theta_{\text{opt}})$.

The book [4] describes perhaps the best-known work—the computer-aided control system package QDES—that combines Youla parametrization and convex optimization for LTI controller design (see also [3]). QDES consists of a front-end compiler that translates a control design problem into problem (15.5); this optimization problem is solved numerically by further reducing it to a quadratic program. In order to reformulate problem (15.5) into a quadratic program, some approximation and sampling of frequency domain constraints is necessary. However, the positive and bounded real lemmas and their variations (see, for example, [1, 19, 14]) can be used to *exactly* formulate a number of frequency domain constraints into LMI constraints. This motivates the use of LMI techniques to solve problem (15.5), which we develop in the rest of the chapter.

15.2.2 Controller design specifications as LMI constraints

We now show how some typical constraints on H_{zw} can be reformulated as LMI constraints. Of course, since quadratic programs can be directly translated into LMI optimization problems [6], every controller design constraint listed in [3] can be reformulated as an LMI constraint. In addition, we will show how certain frequency domain constraints can be naturally reformulated as LMI constraints. We will restrict the Youla parameter Q to lie in the finite-dimensional subspace $\mathcal{Q}_{\text{fin}}$, given in (15.4). The corresponding set of achievable closed-loop maps is

$$\mathcal{H}_{\text{fin}} = \{T_1 + T_2 Q T_3 \mid Q \in \mathcal{Q}_{\text{fin}}\}.$$

Constraints on the response to specific inputs

Suppose that a certain exogenous output (i.e., a component of z) is required to lie within specified upper and lower bounds for a given reference input signal (i.e., a component of w). Let $H_{zw,\text{ref}}$ be the corresponding transfer function. Then the response constraint is simply an *affine* constraint on the $H_{zw,\text{ref}}$ and therefore on Θ (see [3, 4]).

LMIs for asymptotic tracking constraints

Suppose that a certain exogenous output is required to asymptotically track a specific input signal. Let $H_{zw,\text{track}}$ be the corresponding transfer function. Then the tracking constraint is simply an *equality* constraint on $H_{zw,\text{track}}(1)$ and therefore on Θ (see [3, 4]).

LMIs for $\mathbf{H}_2$ norms objectives

The $\mathbf{H}_2$ norm of a transfer function H of a stable linear system is defined as

$$||H||_2 = \sqrt{\frac{1}{2\pi}\int_0^{2\pi} \left|H(e^{j\theta})\right|^2 \, d\theta}.$$

From Parseval's theorem, the $\mathbf{H}_2$ norm can also be calculated as the square root of the sum of the squares of the impulse response coefficients. As the $\mathbf{H}_2$ norm measures the root-mean-square (RMS) value of the output of the system when it is driven by white noise with unit power spectral density, constraints on $||H_{zw}||_2$ provide a way of incorporating noise sensitivity constraints on the design.

Suppose the transfer function H has a state-space realization (A, B, C, D). Then $||H||_2$ can be calculated as follows. Define the controllability Gramian W as the solution to the Lyapunov equation

$$AWA^T - W + BB^T = 0.$$

Then the $\mathbf{H}_2$ norm is

$$||H||_2 = \sqrt{\mathrm{Trace}(CWC^T + DD^T)}.$$

Now consider the constraint that the $\mathbf{H}_2$ norm of the transfer function from some (or all) of the components of w to some (or all) of the components of z be less than some γ. Let this transfer function be denoted $\tilde{H}_{zw}$. Since $H_{zw} \in \mathcal{H}_{\mathrm{fin}}$, the transfer function $\tilde{H}_{zw}$ has a state-space realization $(A_{zw}, B_{zw}, C_{zw}(\Theta), D_{zw}(\Theta))$, where A_{zw} and B_{zw} are real matrices, and C_{zw} and D_{zw} are affine functions of Θ.

Then, the constraint $||\tilde{H}_{zw}||_2 \le \gamma$ is equivalent to

$$A_{zw}WA_{zw}^T - W + B_{zw}B_{zw}^T = 0, \quad \mathrm{Trace}(C_{zw}(\Theta)WC_{zw}(\Theta)^T + D_{zw}(\Theta)D_{zw}(\Theta)^T) \le \gamma^2.$$

This is easily rewritten as the LMI constraint

$$\begin{array}{c} A_{zw}WA_{zw}^T - W + B_{zw}B_{zw}^T = 0, \\ X = X^T, \\ \mathrm{Trace}X \le \gamma^2, \end{array} \quad \begin{bmatrix} X & D_{zw}(\Theta) & C_{zw}(\Theta)W^{\frac{1}{2}} \\ D_{zw}(\Theta)^T & I & 0 \\ W^{\frac{1}{2}}C_{zw}^T & 0 & I \end{bmatrix} \ge 0.$$

LMIs for $\mathbf{H}_\infty$ norms objectives

The $\mathbf{H}_\infty$ norm of a transfer function H of a stable linear system is defined as

$$||H||_\infty = \max_{\theta \in [0, 2\pi]} \sigma_{\max}\left(H(e^{j\theta})\right),$$

where $\sigma_{\max}(M)$ denotes the maximum singular value (spectral norm) of a matrix M. The $\mathbf{H}_\infty$ norm measures the $\mathbf{L}_2$- or energy-gain of the system; therefore, constraints on $||H_{zw}||_\infty$ provide a way of incorporating noise amplification constraints on the design. In addition, $\mathbf{H}_\infty$ constraints provide a way of incorporating robustness requirements into the design; see, for example, [8, 9, 13].

Suppose the transfer function H has a state-space realization (A, B, C, D). Then the bounded real lemma (see [6] and the references therein) enables the reformulation of the constraint $||H||_\infty \le \gamma$ as the following LMI constraint on P:

$$P = P^T, \quad \begin{bmatrix} A^TPA - P + C^TC & A^TPB + C^TD \\ B^TPA + D^TC & B^TPB + D^TD - \gamma^2 I \end{bmatrix} \le 0.$$

Now, consider the constraint that the $\mathbf{H}_\infty$ norm of the transfer function $\tilde{H}_{zw}$ from some (or all) of the components of w to some (or all) of the components of z be less than some γ. Using a state-space realization $(A_{zw}, B_{zw}, C_{zw}(\Theta), D_{zw}(\Theta))$ for $\tilde{H}_{zw}$, where A_{zw} and B_{zw} are real matrices, and C_{zw} and D_{zw} are affine functions of Θ, the constraint $\|\tilde{H}_{zw}\|_\infty \le \gamma$ is equivalent to the existence of $P = P^T$ such that

$$\begin{bmatrix} A_{zw}^T P A_{zw} - P + C_{zw}(\Theta)^T C_{zw}(\Theta) & A_{zw}^T P B_{zw} + C_{zw}(\Theta)^T D_{zw}(\Theta) \\ B_{zw}^T P A_{zw} + D_{zw}(\Theta)^T C_{zw}(\Theta) & B_{zw}^T P B_{zw} + D_{zw}(\Theta)^T D_{zw}(\Theta) - \gamma^2 I \end{bmatrix} \le 0$$

holds. This is easily rewritten as the LMI constraint

$$P = P^T, \quad \begin{bmatrix} A_{zw}^T P A_{zw} - P & A_{zw}^T P B_{zw} & C_{zw}(\Theta)^T \\ B_{zw}^T P A_{zw} & B_{zw}^T P B_{zw} - \gamma^2 I & D_{zw}(\Theta)^T \\ C_{zw}(\Theta) & D_{zw}(\Theta) & -I \end{bmatrix} \le 0. \tag{15.6}$$

The implication of section 15.2.2 is that the problem of LTI controller design with several common design specifications can be posed as an optimization problem (15.5) with LMI constraints (and objective) and solved numerically using standard software tools such as [11, 12]. We demonstrate the application of this approach toward controller design for the NEC Laser Bonder.

15.3 Design of an LTI controller for the NEC Laser Bonder

A laser bonder is a soldering machine that connects the leads of an integrated circuit (IC) chip with pads on the IC board. The bonding head consists of a small tool that presses a lead of the IC on the corresponding pad. Lasers then melt the solder of the pad thereby completing the connection. Once a lead is successfully connected, the tool moves up to its initial position. Then the positioning stage that holds the IC board moves above the next lead, and the process is repeated in order for the new connection to be made.

A schematic model of the bonder head is shown in Figure 15.2. The bonder head consists of a tool, a linear voice coil motor (VCM), which drives the tool up and down, and a position sensor (with a linear scale), which measures the vertical position of the tool. Our objective is the design of a controller that achieves the up–down positioning with high speed and precision.

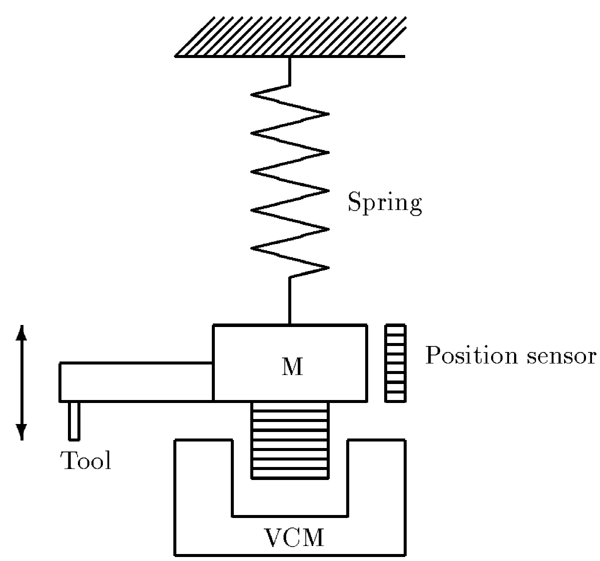

FIG. 15.2. *Schematic model of the NEC Laser Bonder.*

Mass M	1.91 Kg
Resistance R	5.96 Ω
Inductance L	2.25 mH
Spring constant k_s	422 N/m
Thrust force constant k_f	12.8 N/A
Velocity-current coefficient k_e	12.8 V-s/m

TABLE 15.1

Model parameter values for the NEC Laser Bonder.

15.3.1 Modeling of NEC Laser Bonder

The equation governing the motion of the bonder head is

$$M\frac{d^2}{dt^2}h(t) = F(t) - k_s h(t), \tag{15.7}$$

where F is the thrust force of the linear motor, k_s is the spring constant, and h is the tool position. The thrust force is given by $F(t) = k_f i(t)$, where k_f is the thrust force constant and i is the current through the motor. This current, in turn, satisfies

$$V_m(t) = Ri(t) + k_e\frac{d}{dt}h(t) + L\frac{d}{dt}i(t), \tag{15.8}$$

where V_m is the voltage input to the motor, R is the resistance of motor, L is its inductance, and k_e is its velocity-current coefficient. The values of the various constants are shown in Table 15.1.

Equations (15.7) and (15.8) can be combined to yield the following state equation.

$$\frac{d}{dt}\begin{bmatrix} h \\ \dot{h} \\ i \end{bmatrix} = \begin{bmatrix} 0 & 1 & 0 \\ -k_s/M & 0 & k_f/M \\ 0 & -k_e/L & -R/L \end{bmatrix}\begin{bmatrix} h \\ \dot{h} \\ i \end{bmatrix} + \begin{bmatrix} 0 \\ 0 \\ 1/L \end{bmatrix} V_m. \tag{15.9}$$

The controller to be designed has access to the position reference input h_{ref} and the output of the tool position sensor h_{se}, which is simply the actual tool position with some additive sensor noise n_{se}. The control input, i.e, the output of the controller, is a motor voltage V_{in}; this signal, corrupted by an additive noise n_{act}, drives the motor. In addition, there is a disturbance $\tilde{\tau}_d$ that acts on the motor. For convenience, we scale this disturbance by $1/M$ and define $\tau_d = \tilde{\tau}_d/M$.

In our framework, the position reference input h_{ref}, the scaled motor disturbance τ_d, the position sensor noise n_{se}, and the actuator noise n_{act} form the exogenous input w; the computed voltage V_{in} is the control input u; the actual position h and the actual motor input voltage V_m form the regulated variables z; and the reference input h_{ref} and the sensed tool position h_{se} form the measured variable y (see Figure 15.3). From (15.9), we then have

$$\frac{d}{dt}\begin{bmatrix} h \\ \dot{h} \\ i \end{bmatrix} = \begin{bmatrix} 0 & 1 & 0 \\ -k_s/M & 0 & k_f/M \\ 0 & -k_e/L & -R/L \end{bmatrix}\begin{bmatrix} h \\ \dot{h} \\ i \end{bmatrix} + \left[\begin{array}{cccc|c} 0 & 0 & 0 & 0 & 0 \\ 0 & 1 & 0 & 0 & 0 \\ 0 & 0 & 0 & 1/L & 1/L \end{array}\right]\left[\begin{array}{c} h_{ref} \\ \tau_d \\ n_{se} \\ n_{act} \\ \hline V_{in} \end{array}\right].$$

Substituting the parameter values shown in Table 15.1, we have the following state

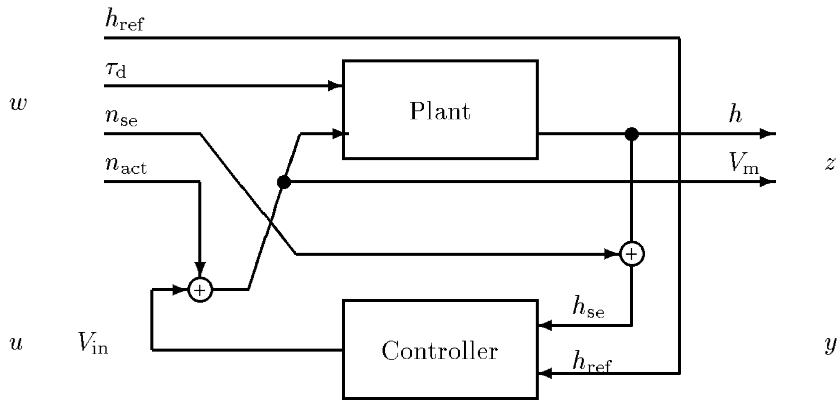

FIG. 15.3. *Block diagram of the NEC Laser Bonder.*

equations that describe a linear model for the Laser Bonder:

$$\frac{d}{dt}\begin{bmatrix} h \\ \dot{h} \\ i \end{bmatrix} = \begin{bmatrix} 0 & 1 & 0 \\ -221 & 0 & 6.7 \\ 0 & -5689 & -2649 \end{bmatrix}\begin{bmatrix} h \\ \dot{h} \\ i \end{bmatrix} + \left[\begin{array}{cccc|c} 0 & 0 & 0 & 0 & 0 \\ 0 & 1 & 0 & 0 & 0 \\ 0 & 0 & 0 & 444 & 444 \end{array}\right]\left[\begin{array}{c} h_{\mathrm{ref}} \\ \tau_{\mathrm{d}} \\ n_{\mathrm{se}} \\ n_{\mathrm{act}} \\ \hline V_{\mathrm{in}} \end{array}\right],$$

$$\left[\begin{array}{c} h \\ V_{\mathrm{m}} \\ \hline h_{\mathrm{se}} \\ h_{\mathrm{ref}} \end{array}\right] = \left[\begin{array}{ccc} 1 & 0 & 0 \\ 0 & 0 & 0 \\ \hline 1 & 0 & 0 \\ 0 & 0 & 0 \end{array}\right]\begin{bmatrix} h \\ \dot{h} \\ i \end{bmatrix} + \left[\begin{array}{cccc|c} 0 & 0 & 0 & 0 & 0 \\ 0 & 0 & 0 & 1 & 1 \\ \hline 0 & 0 & 1 & 0 & 0 \\ 1 & 0 & 0 & 0 & 0 \end{array}\right]\left[\begin{array}{c} h_{\mathrm{ref}} \\ \tau_{\mathrm{d}} \\ n_{\mathrm{se}} \\ n_{\mathrm{act}} \\ \hline V_{\mathrm{in}} \end{array}\right].$$

Discretizing the system with a sampling frequency of 1KHz, we obtain

$$P = \begin{bmatrix} 0 & p_1 & 0 & p_0 & p_0 \\ 0 & 0 & 0 & 1 & 1 \\ 1 & 0 & 0 & 0 & 0 \\ 0 & p_1 & 1 & p_0 & p_0 \end{bmatrix} \begin{array}{c} (h) \\ (V_{\mathrm{m}}) \\ (h_{\mathrm{ref}}) \\ (h_{\mathrm{se}}) \end{array}$$

$$\begin{array}{ccccc} (h_{\mathrm{ref}}) & (\tau_{\mathrm{d}}) & (n_{\mathrm{se}}) & (n_{\mathrm{act}}) & (V_{\mathrm{in}}) \end{array}$$

where

$$p_0(\lambda) = \frac{10^{-7}\left(2.8584\lambda^2 + 6.7588\lambda + 0.7884\right)}{\lambda^3 - 2.0572\lambda^2 + 1.1281\lambda - 0.07072},$$

and

$$p_1(\lambda) = \frac{10^{-7}\left(4.9898\lambda^2 + 4.6278\lambda - 0.3515\right)}{\lambda^3 - 2.0572\lambda^2 + 1.1281\lambda - 0.07072}.$$

15.3.2 Design specifications

There are three main design specifications: high speed, high precision, and high reliability. More precisely, we have the following design constraints.

SP-1 *Tracking a given reference input.* In the absence of disturbances and noises, for the reference input h_{ref}, shown in solid lines in Figure 15.4, the position h is required to lie within the limits shown in dashed lines. This constraint ensures that the design satisfies a number of specifications:

- *Tracking delay.* The delay in tracking the reference input must not exceed 3ms.

- *Settling interval.* The response is required to lie within $\pm 3\mu m$ from $20ms$ onward.
- *Overshoot.* The overshoot must not exceed $3\mu m$.

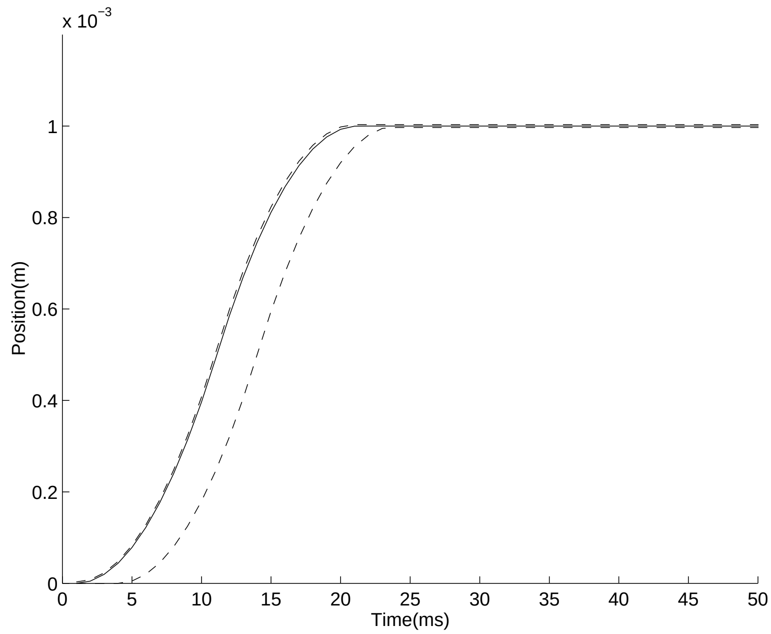

FIG. 15.4. *Constraints on the response to a given reference input. The solid line shows the reference input and the dashed lines the limits within which the response is required to lie.*

SP-2 *Asymptotic tracking.* In the absence of disturbances and noises, the step response from the reference input $h_{\rm ref}$ to the position h must eventually settle at one.

SP-3 *Bounds on input signal $V_{\rm m}$.* In the absence of disturbances and noises, the voltage input V to motor is limited to $\pm 10V$, reflecting the limitations of the transformer driving the motor.

The objective follows:

OBJ Minimize the $\mathbf{H}_\infty$-norm of transfer matrix from reference input ($h_{\rm ref}$) and disturbance (τ_d) to position (h) and motor voltage ($V_{\rm m}$).

This serves to mitigate the effect of disturbances at the signals of interest.

15.3.3 Setting up the LMI problem

The open-loop system is stable, and $K_{\rm nom}$ and $L_{\rm nom}$ can be taken to be zero in order to generate T_1, T_2, and T_3. However, since the open-loop system is very lightly damped (i.e., the poles of the open-loop system were very close to but less than one), we choose the feedback gain $K_{\rm nom}$ and observer gain $L_{\rm nom}$, using standard LQG control, to increase the damping on the system (i.e., the LQG controller served to decrease the magnitude of the poles of the closed-loop system). This step, strictly speaking, is unnecessary; however, our experience has shown that the optimization problems are much better conditioned with this additional step.

The set $\mathcal{Q}$ was chosen as

$$\mathcal{Q} = \left\{ Q = \left[\; (\theta_1 + \theta_2\lambda^{-1} + \theta_3\lambda^{-2} + \theta_4\lambda^{-3}) \qquad (\theta_5 + \theta_6\lambda^{-1} + \theta_7\lambda^{-2} + \theta_8\lambda^{-3}) \; \right] \right\}.$$

This set can be easily rewritten in the form of (15.4), with $\Theta = [\theta_1 \cdots \theta_8]$.

From the argument in section 15.2.2, the specifications **SP-1** and **SP-2** each lead to two linear constraints on Θ; in the notation of problem (15.5), we obtain four LMI constraints $\phi_1, \ldots, \phi_4$. The specification **SP-3** is an equality constraint on Θ, which can be represented in the form of two LMI constraints ϕ_5 and ϕ_6.

The objective **OBJ** is incorporated in problem (15.5) by defining ϕ_7 as the LMI constraint (15.6) and setting $\phi_0 = \gamma^2$.

15.3.4 Numerical results

We used the Matlab LMI Control Toolbox [11] to solve problem (15.5) to obtain Θ_{opt} and thus K_{opt}. Figure 15.5 shows the nominal (i.e., noise- and disturbance-free) response of the closed-loop system with the optimal controller in place. The response lies between the specified upper bound and lower bounds. In particular, the tracking delay, settling interval, and overshoot constraints are satisfied. Moreover, the response converges to the steady-state reference input value of 0.001m.

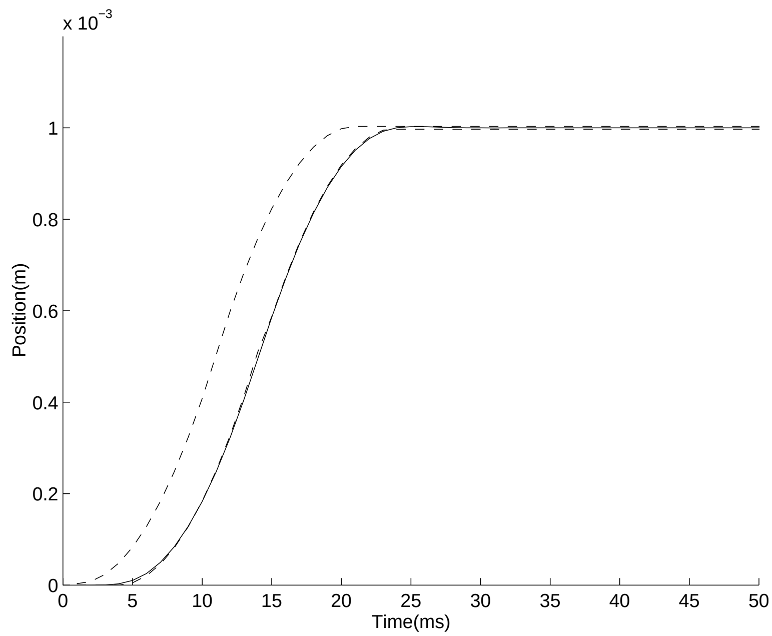

FIG. 15.5. *The response to the reference input, shown in a solid line. The dashed lines show the constraints.*

Figure 15.6 shows the motor voltage V_{m} corresponding to the reference input. Note for all time the magnitude is under 10V, as required.

The optimal value of the objective **OBJ** subject to the constraints **SP-1** through **SP-3**, i.e., the smallest $\mathbf{H}_\infty$-norm from $[h_{\text{ref}} \quad \tau_d]$ to $[h \quad V_{\text{m}}]$ subject to the various design constraints, is 4.4×10^5. For purposes of comparison, we attempted to find the smallest $\mathbf{H}_\infty$-norm achievable with LQG controllers that satisfied the design constraints and obtained a value of 5.8×10^5. Thus the $\mathbf{H}_\infty$ norm with the best LQG controller that we could design is about 20% larger in this example; moreover, there is no systematic way of incorporating multiple design constraints in the LQG design procedure (we had to resort to trial and error). It is possible that a more experienced LQG control designer could match the LMI design; however, this makes the point that with the assistance of the computer-aided procedure presented herein, even inexperienced users can quickly create useful designs.

Next, we study numerically the interaction between two competing constraints, *viz.*,

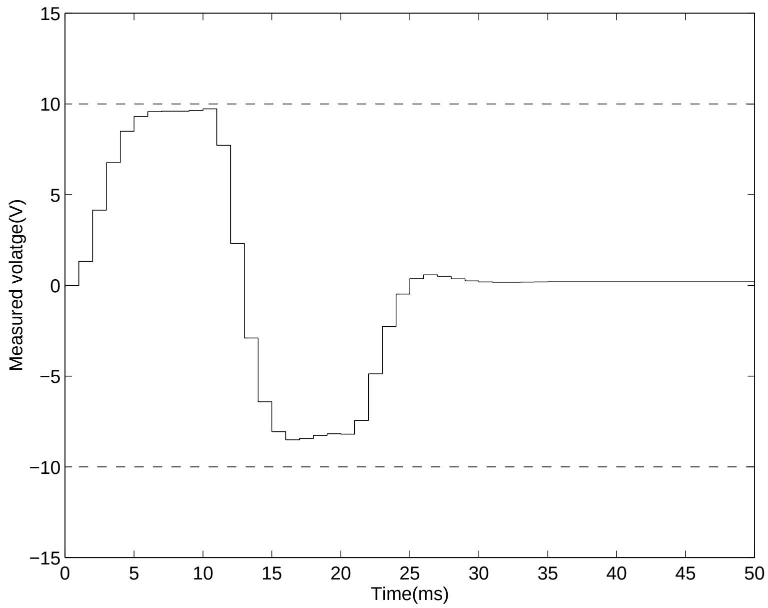

FIG. 15.6. *The measured voltage of the motor to the reference input, shown in a solid line. The dashed lines show the motor voltage constraints.*

the $\mathbf{H}_\infty$ norm of transfer matrix from $[h_{\rm ref} \;\; \tau_d]$ to $[h \;\; V_{\rm m}]$, and the tracking delay. Clearly, increasing the allowable tracking delay, i.e., relaxing the tracking delay constraint, offers the potential of reducing the $\mathbf{H}_\infty$ norm. We study the trade-off between these quantities for three values for the settling interval. The trade-off curves are shown in Figure 15.7. These results show that in the case of a settling interval of $\pm 3\mu m$, the $\mathbf{H}_\infty$-norm does not get smaller when the tracking delay constraint is relaxed beyond 4ms, suggesting that other design constraints are then binding. Similar comments can be made in the case of setting intervals of $\pm 10\mu m$ and $\pm 30\mu m$. As expected, for every value of the tracking delay, the $\mathbf{H}_\infty$ norm decreases when the settling interval is allowed to be larger.

Besides quantifying the interaction between competing constraints, the trade-off curves serve to illustrate the limits of performance of LTI controllers; every point (d, γ) above a trade-off curve is an achievable design specification, meaning that there is an LTI controller that simultaneously satisfies the maximum actuator input and settling interval constraints and results in a closed-loop response that has a tracking delay that does not exceed d, with an $\mathbf{H}_\infty$ norm from $[h_{\rm ref} \;\; \tau_d]$ to $[h \;\; V_{\rm m}]$ that does not exceed γ. Every point below the curve represents an (almost certainly)[1] unachievable design specification.

15.4 Conclusions

We have presented a numerical control design method for designing optimal LTI controllers for LTI plants with multiple design constraints. The techniques combine convex optimization over LMIs with the Youla parametrization of the set of achievable stable closed-loop maps. The advantages of this approach are that engineering specifications can be directly incorporated in the design, without calling on the experience or intuition of the designer to "tune" the design parameters. The particular advantage with the use of LMIs is that several important frequency domain constraints can be exactly reformulated as LMI constraints using the bounded real lemma. In addition to designing controllers, it is possible to study the limits of performance of linear controllers,

[1] Recall that we are restricting Q to lie in the finite-dimensional subspace $Q_{\rm fin}$; hence the parenthetical qualification.

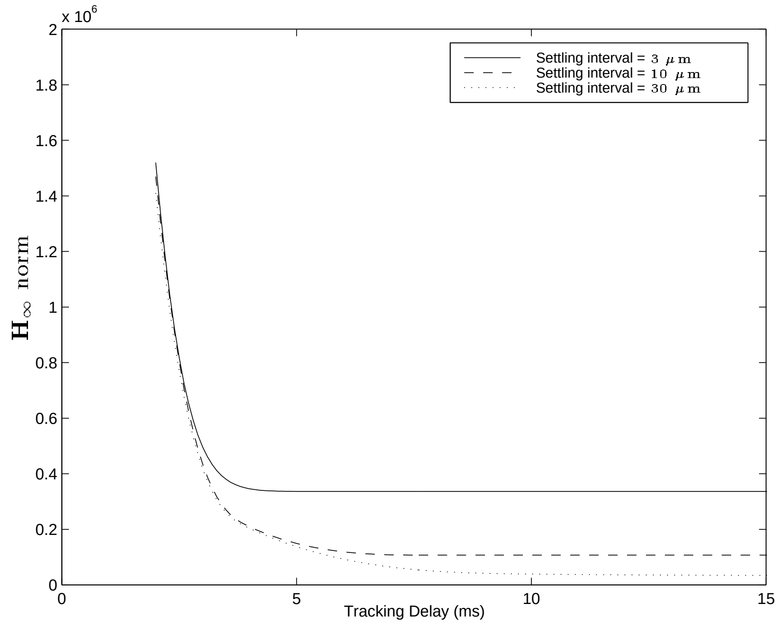

FIG. 15.7. *Tradeoff between the tracking delay and* $\mathbf{H}_\infty$ *norm of the transfer function from* $[h_{\rm ref}\ \ \tau_d]$ *to* $[h\ \ V_{\rm m}]$.

that is, to numerically determine the best achievable performance using linear controllers. We can also study the interaction between competing design constraints by numerically determining trade-off curves.

The task of implementing the controllers presented herein on the "real" NEC Laser Bonder system remains. Another issue that is of interest is the incorporation of robustness requirements on the design so as to account for parameter and operating condition variations.

References

[1] B. Anderson and S. Vongpanitlerd, *Network analysis and synthesis: a modern systems theory approach*, Prentice-Hall, 1973.

[2] V. Balakrishnan and A. Tits, *Numerical optimization-based design*, in Chapter 47, The Control Handbook, W. Levine, ed., CRC Press, 1995, pp. 749–758.

[3] S. Boyd, V. Balakrishnan, C. Barratt, N. Khraishi, X. Li, D. Meyer, and S. Norman, *A new CAD method and associated architectures for linear controllers*, IEEE Trans. Aut. Control, AC-33 (1988), pp. 268–283.

[4] S. Boyd and C. Barratt, *Linear Controller Design: Limits of Performance*, Prentice-Hall, 1991.

[5] S. Boyd, C. Barratt, and S. Norman, *Linear controller design: Limits of performance via convex optimization*, Proc. IEEE, 78 (1990), pp. 529–574.

[6] S. Boyd, L. El Ghaoui, E. Feron, and V. Balakrishnan, *Linear Matrix Inequalities in System and Control Theory*, vol. 15 of Studies in Applied Mathematics, SIAM, Philadelphia, PA, June 1994.

[7] S. Boyd, N. Khraishi, C. Barratt, S. Norman, V. Balakrishnan, and D. Meyer, *QDES Version 1.5*, Information Systems Laboratory, Electrical Engineering Dept., Stanford University, Stanford, CA 94305, 1990.

[8] C. A. Desoer and M. Vidyasagar, *Feedback Systems: Input-Output Properties*, Academic Press, New York, 1975.

[9] J. Doyle, B. Francis, and A. Tannenbaum, *Feedback Control Theory*, Macmillan, 1992.

[10] J. Doyle, K. Glover, P. P. Khargonekar, and B. A. Francis, *State-space solutions to standard* $\mathbf{H}_2$ *and* $\mathbf{H}_\infty$ *control problems*, IEEE Trans. Aut. Control, AC-34 (1989), pp. 831–847.

[11] P. Gahinet and A. Nemirovskii, *LMI Control Toolbox: the LMI Lab*, The MathWorks, Inc., 1995.

[12] L. E. Ghaoui, F. Delebecque, and R. Nikoukhah, *LMITOOL: A User-friendly Interface for LMI Optimization*, ENSTA/INRIA, 1995. Software available via anonymous FTP from `ftp.inria.fr`, under directory `pub/elghaoui/lmitool`.

[13] M. Green and D. J. N. Limebeer, *Linear Robust Control*, Information and System sciences, Prentice Hall, Englewood Cliffs, NJ, 1995.

[14] R. E. Kalman, *Lyapunov functions for the problem of Lur'e in automatic control*, Proc. Nat. Acad. Sci., USA, 49 (1963), pp. 201–205.

[15] D. G. Meyer, V. Balakrishnan, C. Barratt, S. Boyd, N. Khraishi, X. Li, and S. Norman, *Intelligent specification language compilers, the Q-parametrization, and convex programming: Concepts for an advanced computer-aided control system design method*, in Advanced Computing Concepts and Techniques in Control Engineering, M. J. Denham and A. J. Laub, eds., vol. 47 of NATO ASI Series F: Computer and Systems Sciences, Springer-Verlag, Berlin, 1987, pp. 487–496.

[16] S. Norman and S. Boyd, *Numerical solution of a two-disk problem*, in Proc. American Control Conf., 1989, pp. 1745–1747. Reprinted in *Recent Advances in Robust Control*, pages 285-287, edited by P. Dorato and R. K. Yedavalli, IEEE Press.

[17] G. Stein and M. Athans, *The LQG/LTR procedure for multivariable feedback control design*, IEEE Trans. Aut. Control, AC-32 (1987), pp. 105–114.

[18] M. Vidyasagar, *Control System Synthesis: A Factorization Approach*, MIT Press, 1985.

[19] V. A. Yakubovich, *The solution of certain matrix inequalities in automatic control theory*, Soviet Math. Dokl., 3 (1962), pp. 620–623. In Russian, 1961.